EM THEORY MANUAL

# Electromagnetism and Linear Algebra in LS-DYNA

Tested with LS-DYNA® v980 Revision Beta

Thursday 9th August, 2012

LSTC
Livermore Software
Technology Corp.

**Disclaimer:**

LSTC does not warrant that the material contained herein will meet the user's requirements, is error free, or will produce the desired results.

FURTHERMORE, LSTC MAKES NO WARRANTIES, EITHER EXPRESS OR IMPLIED, ORAL OR WRITTEN, WITH RESPECT TO THE DOCUMENTATION AND SOFTWARE DESCRIBED HEREIN INCLUDING, BUT NOT LIMITED TO ANY IMPLIED WARRANTIES (i) OF MERCHANTABILITY, OR (ii) FITNESS FOR A PARTICULAR PURPOSES, OR (iii) ARISING FROM COURSE OF PERFORMANCE OR DEALING, OR FROM USAGE OF TRADE.

From time to time LSTC may at its sole discretion release updates which may include corrections to erroneous material. LSTC encourages users to periodically check this site for updates and to report any errors or inconsistencies encountered to bugs@lstc.com.

| Document Information | |
|---|---|
| Confidentiality | **external use** |
| Document Identifier | LSTC-LS-DYNA-EM-THE-1.1-1 |
| Prepared by | LSTC® Iñaki Çaldichoury |
| Approved by | LSTC® Pierre L'Eplattenier |
| Number of pages | 40 |
| Date created | Thursday 9th August, 2012 |
| Distribution | LS-DYNA® users |

# Contents

# 1 Introduction

## 1.1 Purpose of this Document

A detailed description of the analytical equations solved by the electromagnetism solver is given as well as the numerical methods used. Additional descriptions of the equations used for some of the main features of the solver is also provided. The objective of this document is to offer the reader who wishes to understand and use the electromagnetism solver of LS-DYNA a precise and easy way to understand insight of the formulas, notions and theories employed by the solver.

# 2 Document Information

| Test Case Summary | |
|---|---|
| Confidentiality | external use |
| Test Case Name | Electromagnetism and Linear Algebra in LS-DYNA |
| Test Case ID | ICFD-THE-1.1 |
| Test Case Status | active |
| Test Case Classification | Theory document |
| Metadata | Theory |

Table 1: Test Case Summary

# 3 The Eddy current solver

## 3.1 Notations and physical variables

Table 2 provides the meaning of each symbol and the SI unit of measure while table 3 provides the conventions and operators used :

| Symbol : | Meaning : | Units (S.I) : |
|---|---|---|
| $\vec{E}$ | Electric field | Volt per meter |
| $\vec{B}$ | Magnetic flux density | Tesla |
| $\vec{H}$ | Magnetic field intensity | Amperes per meter |
| $\vec{j}$ | Current density | Amperes per square meter |
| $\vec{j_s}$ | Source current density | Amperes per square meter |
| $\Phi$ | Scalar Potential | Volt |
| $\vec{A}$ | Vector Potential | Tesla meters |
| $\sigma$ | Electrical conductivity | Siemens per meter |
| $\mu$ | Magnetic permeability | Henries per meter |
| $\mu_0$ | Permeability of free space | Henries per meter |
| $\epsilon_0$ | Permittivity of free space | Farads per meter |
| $\rho$ | Total Charge density | Coulombs per cubic meter |
| $\Omega$ and $\partial\Omega = \Gamma$ | Volume and its boundary surface | Cubic and square meters |
| $V, I$ | Voltage, Current | Volt, Ampere |
| $C, q$ | Capacitance, Charge | Farad, Coulomb |
| $R, L$ | Resistance, Inductance | Ohm, Henry |

Table 2: Variables and constants

| | |
|---|---|
| Grad, Curl, Div operators | $\vec{\nabla}$, $\vec{\nabla}\times$, $\nabla\cdot$ |
| Vectors in $\mathbb{R}^3$ | Arrow overhead : $v\vec{e}c$ |
| Matrices | Bold : $\mathbf{P}$ |
| Vectors in FEM/BEM systems | Small : $a_i$ |

Table 3: Operators and conventions

## 3.2 The Maxwell equations

In order to define the equations solved by the Electromagnetism solver, we start with the Maxwell equations :

$$\vec{\nabla} \times \vec{E} = -\frac{\partial \vec{B}}{\partial t} \tag{1}$$

$$\vec{\nabla} \times \vec{H} = \vec{j} + \epsilon_0 \frac{\partial \vec{E}}{\partial t} \tag{2}$$

$$\nabla \cdot \vec{B} = 0 \tag{3}$$

$$\nabla \cdot \vec{E} = \frac{\rho}{\epsilon_0} \tag{4}$$

$$\vec{j} = \sigma \vec{E} + \vec{j_s} \tag{5}$$

$$\vec{B} = \mu_0 \vec{H} \tag{6}$$

The eddy current approximation used here implies a divergence free current density and no charge accumulation thus resulting in $\epsilon_0 \frac{\partial \vec{E}}{\partial t} = 0$ and $\rho = 0$. Equation (2) and (4) in the "Eddy current approximation" give :

$$\tag{7}$$

$$\vec{\nabla} \times \vec{H} = \vec{j} \tag{8}$$

$$\nabla \cdot \vec{E} = 0 \tag{9}$$

$$\nabla \cdot \vec{j} = 0 \tag{10}$$

The divergence condition given by Equation (3) allows writing $\vec{B}$ as :

$$\tag{11}$$

$$\vec{B} = \vec{\nabla} \times \vec{A} \tag{12}$$

with $\vec{A}$ the magnetic vector potential [1]. Equation (1) then implies that the electric field is given by :

$$\vec{E} = -\vec{\nabla}\Phi - \frac{\partial \vec{A}}{\partial t} \tag{13}$$

with $\Phi$ the electric scalar potential.

Equation (12) leaves a mathematical degree of freedom to $\vec{A}$ (if $\vec{A}$ is transformed to a given $\vec{A} + \vec{\nabla}\psi$ then Equation (12) remains valid). Therefore, the introduction of a gauge i.e a particular choice of the scalar and vector potentials is needed. The gauge chosen here is the "generalized Coulomb" gauge :

$$\nabla(\sigma\vec{A}) = 0 \tag{14}$$

Equation (5), (10), (13) and (14) give :

$$\nabla(\sigma\vec{\nabla}\Phi) = 0 \tag{15}$$

Equation (5), (8), (13) and (12) give :

$$\sigma\frac{\partial\vec{A}}{\partial t} + \vec{\nabla}\times(\frac{1}{\mu}\vec{\nabla}\times\vec{A}) + \sigma\vec{\nabla}\Phi = \vec{j_s} \tag{16}$$

Equation (15) and Equation (16) are the two equations constituting the system that will be solved with $\vec{A}$ and $\Phi$ the two unknowns of the problem.

## 3.3 Finite element representation

The electromagnetism equations are solved with a Finite Element Method [8] using a library called "FEMSTER" developed at the Lawrence Livermore National Laboratories [4]. FEMSTER provides discrete numerical implementations of the concepts from differential forms (often referred as Nedelec elements) [14] [15]. These include in particular the exterior derivatives of gradient, curl and divergence, and also the div-grad, curl-curl and grad-div operators. FEMSTER provides four forms of basis functions, called 0-forms, 1-forms, 2-forms and 3-forms, defined on hexahedra, tetrahedra and prisms. Even if tetrahedra and prisms are supported by the solver it is advised to use hexahedra elements whenever possible.

0-forms are continuous scalar basis functions that have a well defined gradient, the gradient of a 0-form being a 1- form. At first order, the degrees of freedom associated with a 0-form are the values of the scalar field at the nodes of the mesh. In our particular case, the 0-forms are used for the discretization of the scalar potential $\Phi$.

1-forms are vector basis functions with continuous tangential components but discontinuous normal components. They have a well defined curl, the curl of a 1- form being a 2-form. At first order, the degrees of freedom of a 1-form are its line integrals along the edges of the mesh. They are used for the discretization of the electric field $\vec{E}$ , the magnetic field $\vec{H}$ and the vector potential $\vec{A}$ .

2-forms are vector basis functions with continuous normal components across elements but discontinous tangential components. They have a well defined divergence, the divergence of a 2-form being a 3-form. At first order, the degrees of freedom of a 2-form are its fluxes across all the facets of the mesh. They are used for the discretization of the magnetic flux density $\vec{B}$ , and the current density $\vec{j}$ .

Finally, the 3-forms are discontinuous scalar basis functions which cannot be differentiated. Their degrees of freedom at first order are their integrals over the elements of the mesh. Figure 1 offers a summary of the different forms at first order on a hexahedra element.

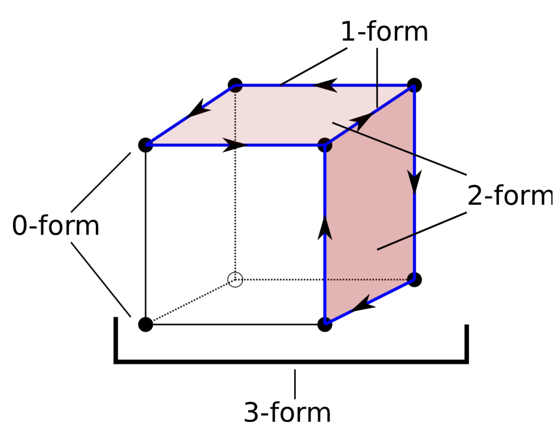


Figure 1: $l$-forms on a hexahedra element

These basis functions define spaces with an exact representation of the De-Rham sequence[3]. They also exactly satisfy numerical relations such as $\vec{\nabla} \times (\vec{\nabla}) = 0$ or $\nabla \cdot (\vec{\nabla}) = 0$, which are very important for conservation laws when solving the systems [16]. At first order, they allow solving partial differential equations at an integrated (Stokes theorem) level which proves to be very efficient and accurate, even on low density meshes, compared to using vector basis functions [16].

The basis functions associated respectively with the 0, 1, 2, and 3- forms will be noted $W_0$, $\vec{W_1}$, $\vec{W_2}$ , and $W_3$. These basis functions define a primal space. In LS-DYNA, this primal space will be constructed by the mesh provided by the user. A dual space can be associated to the primal space. This dual space will not be "physically" represented with solid elements but provides important properties for calculations. In order to introduce this dual space, let's start with their 0-forms that will be defined as the barycenter of the 3-forms of the primal space. The 1-forms of the dual space are the lines connecting the dual 0-forms contained in two adjacent primal 3-forms. The 2-forms of the dual space are the surfaces that cut through the edges of the primal 1-forms. The 3-forms of the dual space are the volumes delimited by the dual 2-forms.

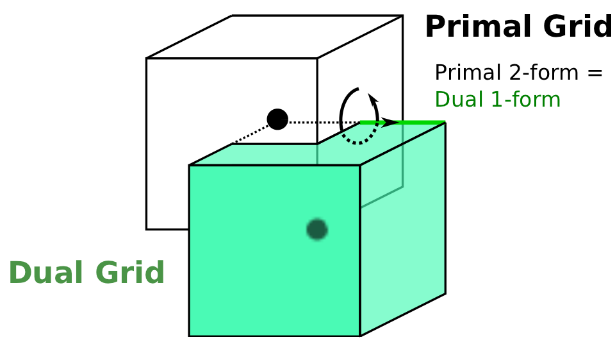


Figure 2: Primal dual spaces

Figure 2 shows the primal and its associated dual space in 3D on hexahedral elements while figure 3 shows the mathematical identities and operators connecting the primal to the dual space where $\mathbf{M}^l$ denotes a $l$-form mass matrix, $\mathbf{S}^l$ denotes a $l$-form stiffness matrix, $\mathbf{T}^{l,m}$ denotes a rectangular topological derivative matrix which maps $l$-forms on m-forms and $\mathbf{D}^{1,m}$ denotes a rectangular derivative matrix which maps $l$-forms on m-forms.

In order to express a 1-form gradient of a 0-form scalar, $\mathbf{T}^{01}$ representing the edge nodal connectivity is defined (at first order) such as :

| Form type : | Associated with : | DOFs : |
|---|---|---|
| 0-form | Nodes | Nodal value |
| 1-form | Edges | Line integral |
| 2-form | Faces | Flux |
| 3-form | Cells | Volume integral |

Table 4: Definition of the $l$-forms

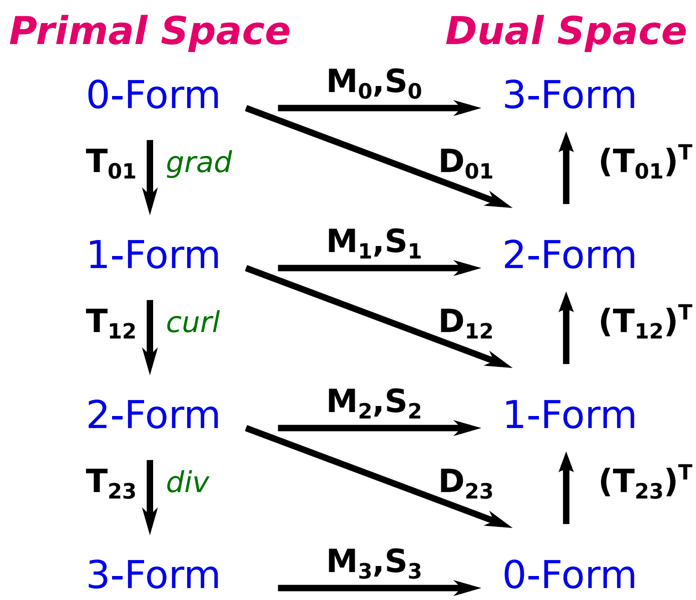


Figure 3: Tonti diagramm

$$\mathbf{T}^{01} = \begin{array}{cc} & \begin{array}{ccccccccc} & & Node(k) & & & & Node(j) & & \end{array} \\ Edge(i) & \begin{pmatrix} \vdots & \vdots & \vdots & \vdots & \vdots & \vdots & \vdots & \vdots & \vdots \\ 0 & \cdots & 1 & \cdots & 0 & \cdots & -1 & 0 & \cdots \\ \vdots & \vdots & \vdots & \vdots & \vdots & \vdots & \vdots & \vdots & \vdots \end{pmatrix} \end{array} \tag{17}$$

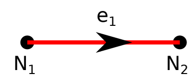


with $Edge(i) = Node(j) \longrightarrow Node(k)$, and $ID_{Node(j)} < ID_{Node(k)}$

In order to express a 2-form curl of a 1-form gradient, the topological derivative matrix $\mathbf{T}^{12}$ representing the face edge connectivity is defined such as :

$$\mathbf{T}^{12} = \begin{array}{cc} & \begin{array}{cccccccccc} Edge(k) & & & Edge(j) & & & & Edge(m) & Edge(n) & \end{array} \\ Face(i) & \begin{pmatrix} \vdots & \vdots & \vdots & \vdots & \vdots & \vdots & \vdots & \vdots & \vdots & \vdots \\ 1 & 0 & \cdots & -1 & \cdots & 0 & \cdots & 1 & -1 & \cdots \\ \vdots & \vdots & \vdots & \vdots & \vdots & \vdots & \vdots & \vdots & \vdots & \vdots \end{pmatrix} \end{array} \tag{18}$$

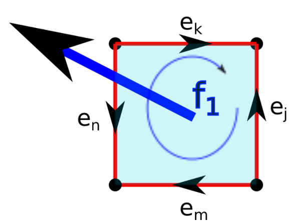


where every face is defined by four edges ( for a hexahedral element). The orientation of the face is based on its flux normal. The signs of the edges on the matrix $\mathbf{T}^{12}$ are adjusted accordingly.

In order to express a 3-form divergence of a 2-form curl, the topological derivative matrix $T^{23}$ representing the element face connectivity is defined such as :

$$\mathbf{T}^{32} = \begin{array}{cc} & \begin{array}{cccccccccc} & & & & Faces & & & & & \end{array} \\ Volume & \begin{pmatrix} \vdots & \vdots & \vdots & \vdots & \vdots & \vdots & \vdots & \vdots & \vdots & \vdots \\ \pm 1 & \pm 1 & \pm 1 & \pm 1 & \cdots & 0 & \cdots & \pm 1 & \pm 1 & \cdots \\ \vdots & \vdots & \vdots & \vdots & \vdots & \vdots & \vdots & \vdots & \vdots & \vdots \end{pmatrix} \end{array} \tag{19}$$

where every volume is defined by its six faces (for a hexahedral element). Depending on the faces' normal orientations, the signs are adjusted accordingly.

The following matrix identities hold [16] :

$$\begin{aligned}
\mathbf{T}^{1,2}\mathbf{T}^{0,1} &= 0\ (Curl - Grad\ Identity) \qquad (20)\\
\mathbf{T}^{2,3}\mathbf{T}^{1,2} &= 0\ (Div - Curl\ Identity) \qquad (21)
\end{aligned}$$

The derivative matrices are mesh dependent and can be written as a product of the topological derivative matrices and an appropriate mass matrix as follows [16] :

$$\begin{aligned}
\mathbf{D}^{0,1} &= \mathbf{M}^{1}\mathbf{T}^{0,1} \qquad (22)\\
\mathbf{D}^{1,2} &= \mathbf{M}^{2}\mathbf{T}^{1,2} \qquad (23)\\
\mathbf{D}^{2,3} &= \mathbf{M}^{3}\mathbf{T}^{2,3} \qquad (24)
\end{aligned}$$

The various stiffness matrices are discrete representations of the standard second order operators from vector calculus such as the Laplacian (or Div-Grad) and the Curl-Curl operators. They can also be written as products of mass and topological derivative matrices as follows :

$$\begin{aligned}
0 - form\ (Div - Grad)\ :\ \mathbf{S}^{0} &= (\mathbf{T}^{0,1})^{T}\mathbf{M}^{1}\mathbf{T}^{0,1} \qquad (25)\\
1 - form\ (Curl - Curl)\ :\ \mathbf{S}^{1} &= (\mathbf{T}^{1,2})^{T}\mathbf{M}^{2}\mathbf{T}^{1,2} \qquad (26)\\
2 - form\ (Grad - Div)\ :\ \mathbf{S}^{2} &= (\mathbf{T}^{2,3})^{T}\mathbf{M}^{3}\mathbf{T}^{2,3} \qquad (27)
\end{aligned}$$

Each of these matrices will have dimensions equal to the number of $l$-form degrees of freedom.

## 3.4 The "Finite Element Method" (FEM) system

Equation (15) is projected on the $W^0$ forms and Equation (16) is projected on the $\vec{W}^1$ forms giving after integrating by part the following weak formulations [16] :

$$\int_\Omega \sigma \vec{\nabla}\Phi \cdot \vec{\nabla} W^0 d\Omega = 0 \tag{28}$$

$$\int_\Omega \sigma \frac{\partial \vec{A}}{\partial t} \cdot \vec{W}^1 d\Omega + \int_\Omega \frac{1}{\mu} \vec{\nabla} \times \vec{A} \cdot \vec{\nabla} \times \vec{W}^1 d\Omega = -\int_\Omega \sigma \vec{\nabla}\Phi \cdot \vec{W}^1 d\Omega + \int_\Gamma \frac{1}{\mu} [\vec{n} \times (\vec{\nabla} \times \vec{A})] \cdot \vec{W}^1 d\Gamma \tag{29}$$

with $d\Omega$ an element of volume $\Omega$ and $\Gamma = \partial\Omega$ the surface of $\Omega$ with $\vec{n}$ outer normal to $\Gamma$.

The $\Phi$ and $\vec{A}$ decompositions on respectfully $W^0$ and $\vec{W}^1$ give :

$$\Phi = \sum \phi_i w_i^0 \tag{30}$$

$$\vec{A} = \sum a_i \vec{w}_i^1 \tag{31}$$

When replacing $\Phi$ and $\vec{A}$ in Equation (28) and (29) by (30) and (31), one gets :

$$\mathbf{S}^0(\sigma)\phi = 0 \tag{32}$$

$$\mathbf{M}^1(\sigma)\frac{\partial a}{\partial t} + \mathbf{S}^1(\frac{1}{\mu})a = -\mathbf{D}^{01}(\sigma)\phi + \mathbf{S}a \tag{33}$$

with :

- The Stiffness matrix of the 0-forms :

$$\mathbf{S}^0(\sigma)(i,j) = \int_\Omega \sigma \vec{\nabla} \times W_i^0 \cdot \vec{\nabla} W_j^0 d\Omega \tag{34}$$

- The Mass matrix of the 1-forms :

$$\mathbf{M}^1(\sigma)(i,j) = \int_\Omega \sigma \vec{W}_i^1 \cdot \vec{W}_j^1 d\Omega \tag{35}$$

- The Stiffness matrix of the 1-forms :

$$\mathbf{S}^1(\frac{1}{\mu})(i,j) = \int_\Omega \frac{1}{\mu} (\vec{\nabla} \times \vec{W}_i^1) \cdot (\vec{\nabla} \times \vec{W}_j^1) d\Omega \tag{36}$$

- The Derivative matrix of the 0-1-forms :

$$\mathbf{D}^{01}(\sigma)(i,j) = \int_\Omega \sigma \vec{\nabla} W_i^0 \cdot (\vec{W}_j^1) d\Omega \tag{37}$$

- The Outside stiffness matrix :

$$\mathbf{S}(\frac{1}{\mu})(i,j) = \int_\Gamma \frac{1}{\mu}[\vec{n} \times (\vec{\nabla} \times \vec{W}_i^1)] \cdot \vec{W}_j^1 d\Gamma \quad (38)$$

Equation (32) and (33) form the FEM system with $\phi$ and $a$ the unknowns. From this system only the outside stiffness matrix can not be directly computed. The calculation of this matrix will be made possible through the definition of a BEM system [18].

## 3.5 The "Boundary Element Method" (BEM) system

In order to solve Equation (38), an intermediate "surface current" variable $\vec{K}$ is introduced producing the same $\vec{A}$ (and thus $\vec{B}$) in the air as the actual volume current. From the Biot-Savart equation :

$$\vec{A}(\vec{x}) = \frac{\mu_0}{4\pi}\int_{\Gamma_y}\frac{1}{|\vec{x}-\vec{y})|}\vec{K}(\vec{y})d\Gamma_y \tag{39}$$

for $\forall x \in \Omega_{air}$ (and thus for $x \in \Gamma$)

It can be shown [13] from Equation (39) that :

$$[\vec{n}\times(\vec{\nabla}\times\vec{A})](\vec{x}) = \frac{\mu_0}{2}\vec{K}(\vec{x}) + \frac{\mu_0}{4\pi}\int_{\Gamma_y}\frac{1}{|\vec{x}-\vec{y})|^3}\vec{n}\times[(\vec{x}-\vec{y})\times\vec{K}(\vec{y})]d\Gamma_y \tag{40}$$

By projecting Equation (39) and $\vec{K}$ on the "twisted" 1-form basis $\vec{V}^1 = \vec{n}\times\vec{W}^1$ and equation (40) against $\vec{W}^1$ one gets :

$$\mathbf{P}k = \mathbf{D}a \tag{41}$$

$$\mathbf{S}a = \mathbf{Q}k = \mathbf{Q}_s k + \mathbf{Q}_d k \tag{42}$$

with :

- The BEM matrix $D$

$$\mathbf{D}(i,j) = \int_{\Gamma_x}\vec{V}_i(\vec{x})\cdot\vec{W}_j(\vec{x})\ d\Gamma_x \tag{43}$$

- The BEM matrix $P$

$$\mathbf{P}(i,j) = \int_{\Gamma_x}\int_{\Gamma_y}\frac{1}{|\vec{x}-\vec{y}|}\vec{V}_i(\vec{x})\cdot\vec{V}_j(\vec{y})\ d\Gamma_x d\Gamma_y \tag{44}$$

- The BEM matrix $Q_S$

$$\mathbf{Q}_s(i,j) = \int_{\Gamma_x}\vec{W}_i(x)\cdot\vec{V}_j(x)\ d\Gamma_x \tag{45}$$

- The BEM matrix $Q_D$

$$\mathbf{Q}_d(i,j) = \int_{\Gamma_x}\int_{\Gamma_y}\frac{1}{|\vec{x}-\vec{y}|^3}\vec{W}_i(x)\cdot\left(\vec{n_x}\times\left[(\vec{x}-\vec{y})\times\vec{V}_j(y)\right]\right)\ d\Gamma_x d\Gamma_y \tag{46}$$

with $\vec{n}_x$ the outer normal at point $x$.

Equation (41) and (42) form the BEM system with $k$ and $a$ the unknowns defined on $\Gamma$.

The matrices $\mathbf{P}$ and $\mathbf{Q}_d$ become singular or nearly singular as $x \to y$ , i.e. for self face integrals or integrals over neighbor faces with a common edge or a common node. Special methods have been included such as the ones described in [22] and [17]. These methods also allow more accurate integration on inhomogeneous faces, i.e. faces with large aspect ratios.

## 3.6 Coupling the FEM with the BEM

The time integration of Equation (33) is done with an implicit backward Euler method :

$$[\mathbf{M}^1(\sigma) + dt\mathbf{S}^1(\frac{1}{\mu})]a^{t+1} = \mathbf{M}^1(\sigma)a^t - dt\mathbf{D}^{01}(\sigma)\phi^{t+1} + dt\mathbf{S}a^{t+1} \tag{47}$$

We note that the BEM term $dt\mathbf{S}\ a^{t+1}$ is implicit ($a^{t+1}$ and not $a^t$) in order to improve the stability. Starting from an initial $\vec{A}$ provided by the FEM defined on the surface, the BEM system gives the outside term $dt\mathbf{S}a^{t+1}$. Consequently, the FEM-System can be solved and a new vector potential $a$ can be calculated. This iterative process consists in solving Equation (47) coupled with (41) (42) resulting in the following global system :

$$\mathbf{P}k_{n+1}^{t+1} = \mathbf{D}a_n^{t+1} \tag{48}$$

$$[\mathbf{M}^1(\sigma) + dt\mathbf{S}^1(\frac{1}{\mu})]a_{n+1}^{t+1} = \mathbf{M}^1(\sigma)a^t - dt\mathbf{D}^{01}(\sigma)\phi^{t+1} + dt\mathbf{Q}k_{n+1}^{t+1} \tag{49}$$

Equation (32) is only solved when a voltage is imposed on the system. Otherwise $\phi = 0$.

The user can either define the time step manually or let the solver estimate a time step value automatically. It is computed as the minimal elemental diffusion time step over the elements. Based on Equation (16), the elemental diffusion time step for a given element reads:

$$dt_{timestep} = \frac{l_e^2}{2D} \tag{50}$$

where D is the diffusion coefficient $D = \frac{1}{\mu_0\sigma}$ and $l_e$ is the minimal edge length of the element (minimal size of the element).

### 3.7 Computation of the EM fields

Once the FEM-BEM system is solved (see Equation (48) and (49)) and the scalar potential $\phi_0$ and the vector potential $a_1$ have been determined, the EM fields can be computed. In this section, the indices 0,1,2 or 3 will be introduced on the vectors for emphasis on the form presenting them (exemple : $\phi_0$ is a 0-form and $a_1$ is a 1-form)

From Equation (13), the electric field is expressed as a 1-form :

$$e_1 = -\mathbf{T}^{01}\phi_0 - \frac{da_1}{dt} \tag{51}$$

with $\mathbf{T}^{01}$ the topological derivative matrix defined in Equation (17) transforming the 0-form $\phi_0$ into the 1-form by representing its gradient : $\mathbf{T}^{01}\phi_0$.

From $e_1$ and Equation (4), the current density can be expressed as a 1-form :

$$j_1 = \sigma e_1 \tag{52}$$

However, the current density represents a flux and needs therefore to be expressed as a 2-form ( so that $\nabla \cdot \vec{j} = 0$ ). The so-called Hodge matrix [10] permits the transformation of a 1-form variable defined in the primal space in a 2-form variable defined in the dual space :

$$e_2 = \mathbf{H}^{12}e_1 \tag{53}$$

From Figure (3) we then have :

$$\mathbf{M}^2(\sigma)j_2 = e_2 \tag{54}$$

with $j_2$ defined in the primal space.

The magnetic flux density is the curl of the vector potential and is therefore expressed as a 2-form :

$$b_2 = -\mathbf{T}^{12}a_1 \tag{55}$$

Finally the following forces and energies can be computed at the element level :

$$\vec{F}_{Lorentz} = \vec{j}_1 \times \vec{B}_2 \tag{56}$$

$$E_{JouleHeating} = \frac{j_2^2}{\sigma} \tag{57}$$

$$E_{Magnetic} = \frac{b_2^2}{2\mu_0} \tag{58}$$

All EM fields are then evaluated at the center of elements as $\mathbb{R}^3$ vector fields for output purposes.

## 3.8 Watching and interpreting the analysis

### 3.8.1 When setting up the problem

Several keywords and options are directly accessible for the user who wishes to control and modify the way the previously described equations will be solved.

- The EM SOLVER BEMMAT card:

  For both matrices $\mathbf{P}$ and $\mathbf{Q}$ of the BEM system defined by equation (41) and (42), a domain decomposition of the mesh is done by the solver inducing a block decomposition of the BEM matrix. The solver then automatically applies a low-rank matrix approximation on every block where it is memory-cost effective. This means that every block $\mathbf{M}_{m,n}$ of $\mathbf{P}$ and $\mathbf{Q}$ will be decomposed as :

  $$\mathbf{M}_{m,n} = \mathbf{U}_{m,r}\mathbf{S}_{r,r}\mathbf{V}_{r,n} \tag{59}$$

  where $\mathbf{S}_r$ is a diagonal matrix of size $r$ containing only the $r$ largest singular values in decreasing order (the other singular values will be replaced by zero) and $\mathbf{U}$ and $\mathbf{V}$ are orthogonal. The user can then choose for each matrix the tolerance that should be applied as a cut off to the singular values :

  $$s_{r,r} \leq (tol) \times s_{1,1} \tag{60}$$

  The user should be aware that $\mathbf{P}$ is symmetric whereas $\mathbf{Q}$ is not. Moreover, $\mathbf{Q}$ is expressed on the edges instead of on the nodes for $\mathbf{P}$ (see Section 4.1.2) and the number of surface edges is approximately equal to two times the number of surface nodes, hence decreasing the tolerance for $\mathbf{Q}$ will most likely be more memory costly then decreasing the tolerance for $\mathbf{P}$. Also, from equations (48) and (49), $\mathbf{P}$ is used to solve a system which sometimes requires low enough tolerances.

- The EM SOLVER BEM and EM SOLVER FEM cards:

  This two cards works in similar ways and act on the BEM system (equation (41)) and on the FEM system (equation (49)). The following description will use equation (41) for illustration. Equation (41) implies finding $k$ such as $\mathbf{P}k = \mathbf{D}a$ The options available are :

  - Solver type : The user can choose between a direct solve, which implies a factorization of $\mathbf{P}$. The matrix needs to be dense or sparse (no block decomposition). This method is no longer used to solve the BEM system, however, it still is the one mostly used in the FEM case. The other option (now default) is to use a Pre-Conditioned Gradient Method (PCG). In the BEM, this allows to have block matrices with low rank blocks and thus to reduce the memory.

- The number of iterations and tolerance when solving the linear system using the Pre-Conditioned Gradient Method. The tolerance value is defined such as :

$$||\mathbf{D}a - \mathbf{P}k|| \leq (tol) \times ||\mathbf{D}a|| \tag{61}$$

- Choice of a preconditioner : If using the Pre-Conditioned method, a preconditioner matrix may be defined. During the iteration process, this matrix will have to be inverted. A system with a preconditioner that is as close to **P** as possible (such as the Broad Diagonal block including all neighbor faces instead of the Diagonal line) will converge in less iterations but each iteration will cost more time due to the inversion process [5].
- Choice of the initial solution. In order to solve the linear system, it may be possible to use as an initial solution the previous solution obtained. If the solution vector is assumed to be nearly parallel to the previous solution vector, like it often happens in time domain eddy-current problems, then the number of iterations will be reduced resulting in a reduction of calculation times.

• The EM SOLVER FEMBEM card:

This card allows the user to define the maximum number of iterations when solving the coupled FEM-BEM system defined by equations (48) and (49) as well as the tolerance. The tolerance criteria is defined such as the two following conditions are met :

$$||k_{n+1}^{t+1} - k_n^{t+1}|| \leq (tol) \times k_n^{t+1} \tag{62}$$

$$||a_{n+1}^{t+1} - a_n^{t+1}|| \leq (tol) \times a_n^{t+1} \tag{63}$$

### 3.8.2 When the analysis is running

When the analysis is running, the EM OUTPUT card provides several level of electromagnetic related output for the user who wishes to analyze the convergence of the different systems and their matrix assembly. The MATS variable gives the level output to the terminal and the MATF variable gives the level output to the messag file. The different levels are :

• Level 0 :

- Only the electromagnetic time step is given without any additional information.

• Level 1 or 2 :

- The assembly of the FEM matrices defined in figure (3) and equation (34), (35), (36) and (37) as well as the assembly of the BEM matrices **P** and **Q** (see equation (44), (45) and (46)) is given.

- Information on every FEM-BEM system (defined in equation (48) and (49)) iteration is given : the norm of the vector potential $a$ (noted $ah$) and the difference between its current and previous iteration value (noted $\%v$), the norm of the surface current variable $k$ (noted $ks$) and the difference between its current and previous iteration value (noted $\%v$), the number of iterations of the BEM system defined in equation (41) (noted $pcgIt$) and the total number of iterations for the BEM system (noted $tot$) since the beginning of the analysis.

- Level 3 :
  - Additional information on the FEM and BEM matrices (number of degrees of freedom, sizes and assembly completion percentage).
  - Convergence of the FEM system defined in equation (33) and number of iterations needed (noted $numPcgIterLoc$) (Only when using PCG method for solving the FEM system).
  - Convergence of the BEM system defined in equation (41) and number of iterations needed (noted $numPcgIterLoc$ same as $pcgit$).

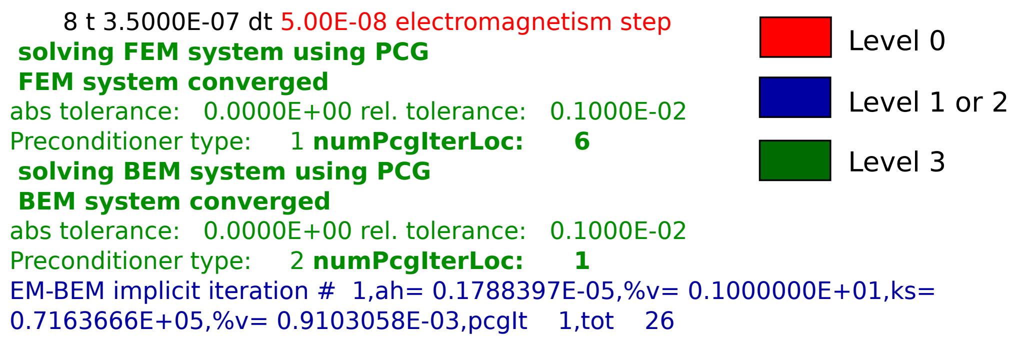


Figure 4: Convergence of the systems-Terminal output

Figure (4) and (5) offer a view of the maximum terminal output.

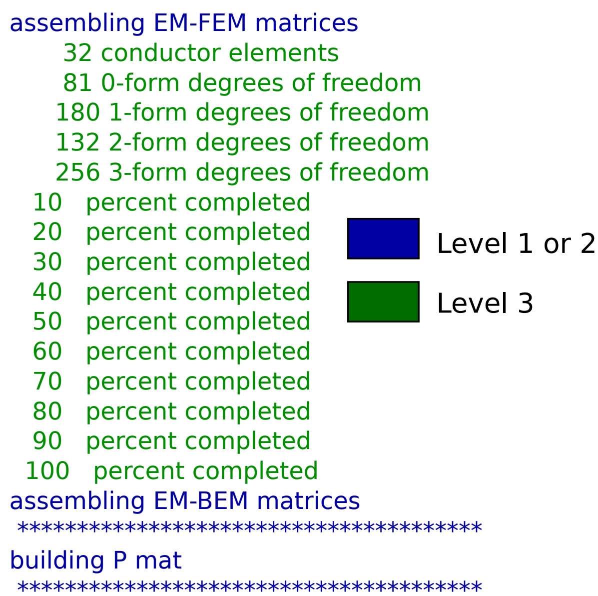


Figure 5: Matrices assembly steps-Terminal output

# 4 Eddy current solver coupling

## 4.1 With an external circuit

### 4.1.1 Imposed tension

The typical problem usually involves a conductive coil that generates induced current in a workpiece (simulation zone of Figure (6)). The source currents generated in the coil are due to the imposition of boundary conditions. It is possible to have an imposed current or an imposed voltage.

If the voltage is imposed, then Equation (32) is solved applying Dirichlet and Newman boundary conditions. No further constraint is applied on the BEM.

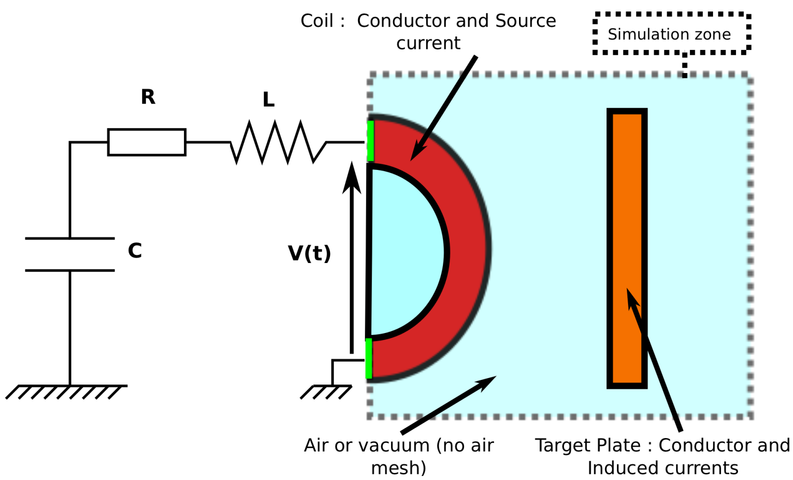


Figure 6: Typical problem with (R,L,C) circuit (Imposed Voltage) on the coil

Three types of circuits can be defined in the EM CIRCUIT card that allow an imposed voltage :

- Type 3 : A circuit equation gives $V(t)$ depending on $R$,$L$, and $C$ (Circuit R,L,C described in Figure (6)) as well as the mesh resistance and inductance/mutuals.
- Type 2 : $V(t)$ is directly given by a user defined load curve
- Type 12 : $V(t)$ follows a sinusoidal behavior defined by its amplitude, frequency and initial time.

### 4.1.2 Imposed current

If the current is imposed (EM circuit card : Type 1 (user defined load curve as for Type 2) and Type 11 (sinusoidal behavior as in Type 12)) as in Figure (7), then $\Phi = 0$, but the

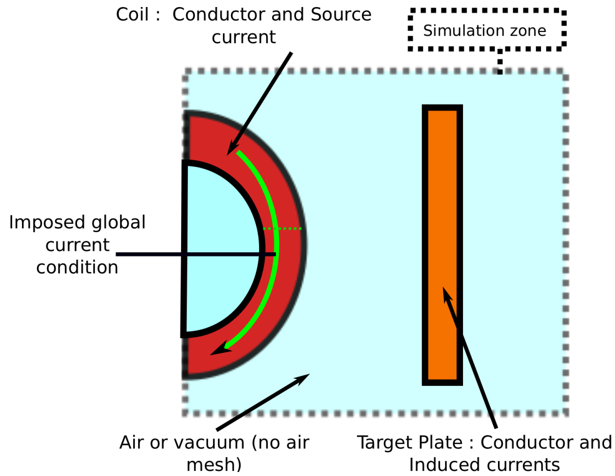


Figure 7: Typical problem with current imposed on the coil

BEM matrix **P** defined in Equation (44) will have additional constraints. Let us introduce the definition of the following sets :

- HE is the set of volume edges.
- BE is the set of surface edges (BEM edges), with size the number of boundary edges,
- BF is the set of surface faces (BEM faces), with size the number of boundary faces,
- BN is the set of surface nodes (BEM nodes), with size the number of boundary nodes.

Let us build the matrix **P** defined in Equation (44). A first possibility would be to define **P** as in Equation (44) using the vector basis $\vec{V_1}$ in order to solve the BEM linear system defined by Equation (41). As the solution vector $k$ must verify the divergence free condition (no charge accumulation on the surface) an additional divergence free constrain must be applied :

$$\mathbf{P}_{BE,BE}\, k_{BE} = \mathbf{D}_{BE,HE}\, a_{HE} \tag{64}$$

$$with\ \mathbf{C}_{BF,BE}\, k_{BE} = 0 \tag{65}$$

with $\mathbf{C}_{BF,BE}$ the surface divergence free constraint matrix $\mathbf{C}_{BF,BE}$ (sparse), with $\mathbf{C}_{i,j} = +1$ or $-1$ if edge $i$ is on face $j$ and $\mathbf{C}_{i,j} = 0$ if not.

This method requires the **P** matrix to be dense and proved to be impractical when solving large systems. It is therefore no longer used. Instead, the matrix **P** is built in a full divergence free space. This way, the constraints introduced by Equation (65) will be directly implemented. A new basis called loop vector basis $\vec{L_i}$ [20] [21] is defined in BE as a linear combination of all of the $\vec{V_k}$s such as edge $k$ contains node $i$, with coefficients equal to 1 or

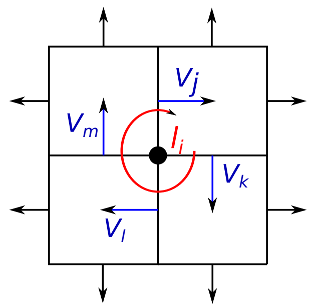


Figure 8: The new loop vector basis in BE

-1 depending on the orientations of the edge ($l_i = \pm v_j \pm v_k \pm v_l \pm v_m$), in order to make $l_i$ loop around node $i$ (See Figure (8)). This base automatically satisfies the divergence-free condition. Therefore, from this new basis, we can define an operator similar to a surface gradient operator $\mathbf{G}_{BE,BN}$ that associates nodes from the nodal space BN to the edge space BE with the important property :

$$\mathbf{C}_{BF,BE}\ \mathbf{G}_{BE,BN} = 0 \tag{66}$$

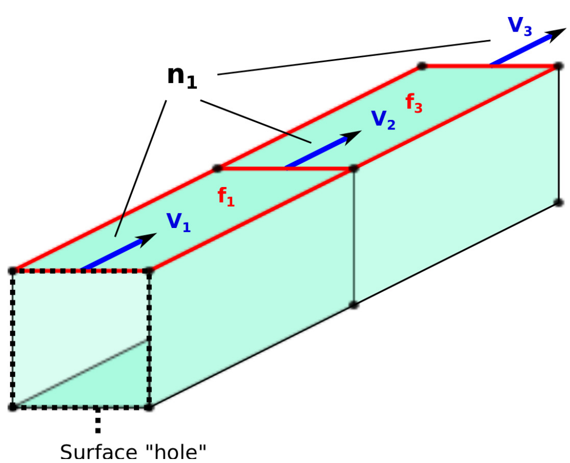


Figure 9: Surface mesh of a conductor. The vector $n_1$ made of $V_1$, $V_2$, and $V_3$ belongs to $Ker(C)$ (the flux entering $f_1$ and $f_2$ is equal to the flux leaving), without belonging to the vector base made of the loop vectors $l_i$

Equation (66) implies $Im(G) \subset Ker(C)$ but not necessarily $Im(G) = Ker(C)$ , therefore in BE, there may exist some vectors combinations of edges that are included in the null space of $C$ (divergence free) without being a gradient ($\notin Im(G)$) [20] . An example of such a vector is described in Figure (9). The dimension of the subspace of edge vectors that are divergence free without being a gradient is written as $\beta_1$. This number is important because it will represent the number of extra non local vectors that will have to be added to the loop vectors in order to describe the full divergence free space where the matrix **P** will be built. Figure (10) offers a sketch of the complete **P** matrix built in the full divergence free space.

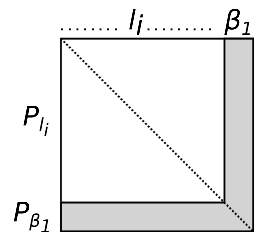


Figure 10: The complete P matrix satisfying the divergence free condition

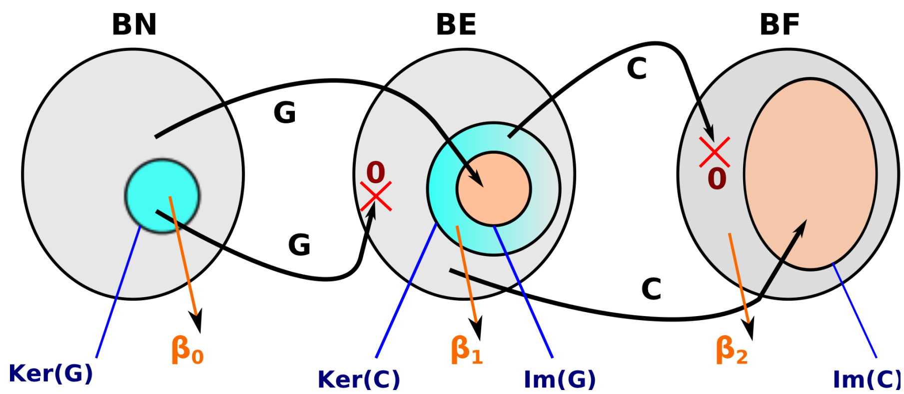


Figure 11: Topology of the different surface base spaces

Figure (11) offers a summary of the topology used [7]. The rank-nullity theorem applied to BE, and BN yields :

$$dim(BN) = dim(Ker(G)) + dim(Im(G)) \tag{67}$$
$$dim(BE) = dim(Ker(C)) + dim(Im(C)) \tag{68}$$

From Equation (67) and (68), we get :

$$\begin{aligned} &dim(BF) - dim(BE) + dim(BN) = \\ &dim(Ker(G)) - (dim(Ker(C)) - dim(Im(G)) + (dim(BF) - dim(Im(C)) \end{aligned} \tag{69}$$

This decomposition allows to define the 3 ”Betti numbers” [2] [12] :

$$\beta_0 = dim(Ker(G)) \tag{70}$$
$$\beta_1 = dim(Ker(C)) - dim(Im(G)) \tag{71}$$
$$\beta_2 = dim(BF) - dim(Im(C)) \tag{72}$$

- On each connected part, the null space of G is of dimension 1, generated by the node vector :

$$\begin{array}{c} n_1 \\ n_2 \\ n_3 \\ \vdots \\ n_n \end{array} \begin{pmatrix} 1 \\ 1 \\ 1 \\ \vdots \\ 1 \end{pmatrix} \alpha \tag{73}$$

  For every conductor part, the dimension of $Ker(G)$ is therefore equal to one. $\beta_0$ is therefore equal to the number of connected parts in the surface mesh.

- $\beta_2$ corresponds to the dimension of the subspace of the face vectors which cannot be reached as the divergence of an edge vector. When there is no hole in the surface ($A = 0$) then every face vector can be defined as any combination of edge vectors except one that will be constrained by the adjacent edge values previously defined. Therefore if $A = 0$ then $\beta_2 = 1$. If the surface isn't closed as in Figure (9) ($A \geq 1$) then $\beta_2 = 0$.

- $\beta_1$ has been previously described and corresponds to the number of constraints that can be added to the **P** matrix. For any given mesh, it is possible to calculate $\beta_0$, $\beta_2$, $dim(BF)$ (Number of surface faces), $dim(BE)$ (Number of surface edges) and $dim(BN)$ (Number of surface nodes). Applying Equation (69), it is possible to calculate $\beta_1$. Physically, $\beta_1$ corresponds to the number of "paths" that the global current can take in a given conductor part. If the user imposes a source current as a circuit boundary condition, then the corresponding constraint will be added to **P**. The user can not define more source current circuits then the value of $\beta_1$ or the system will be overconstrained.

  The solver automatically calculates the number of faces, nodes and edges per conductor surface, the value of $\beta_1$ and $\beta_2$ and writes this data in the messag file. A good way for the user to check his analysis is to determine if Equation (69) is correctly calculated by the solver and if the calculated value of $\beta_1$ corresponds to his expected value (it can be shown that $\beta_1 = 2$ in a torus and $\beta_1 = 1$ in a open conductor as in Figure (9) and $\beta_1 = 0$ in a sphere) (see "Cohomology" section in the messag file) .

## 4.2 With an imposed exterior field

When an exterior field is imposed on the system, then the vector potential becomes :

$$\vec{A} = \vec{A}_0 + \vec{A}_r \tag{74}$$

with $\vec{A}_0$ the external imposed field and $\vec{A}_r$ the reaction field of the conductor.

Assuming that no source current is present then Equation (16) writes :

$$\sigma \frac{\partial \vec{A}}{\partial t} + \vec{\nabla} \times (\frac{1}{\mu} \vec{\nabla} \times \vec{A}) = 0 \tag{75}$$

Similarly to Equation (16), Equation (75) is projected on the $\vec{W}^1$ forms and we get :

$$\int_\Omega \sigma \frac{\partial \vec{A}}{\partial t} \cdot \vec{W}^1 d\Omega + \int_\Omega \frac{1}{\mu} \vec{\nabla} \times \vec{A} \cdot \vec{\nabla} \times \vec{W}^1 d\Omega = \int_\Gamma \frac{1}{\mu} [\vec{n} \times (\vec{\nabla} \times \vec{A})] \cdot \vec{W}^1 d\Gamma \tag{76}$$

with :

$$\begin{aligned} &\int_\Gamma \frac{1}{\mu} [\vec{n} \times (\vec{\nabla} \times \vec{A})] \cdot \vec{W}^1 d\Gamma = \\ &\int_\Gamma \frac{1}{\mu} [\vec{n} \times (\vec{\nabla} \times \vec{A}_0)] \cdot \vec{W}^1 d\Gamma + \int_\Gamma \frac{1}{\mu} [\vec{n} \times (\vec{\nabla} \times \vec{A}_r)] \cdot \vec{W}^1 d\Gamma = \\ &\int_\Gamma \frac{1}{\mu} [\vec{n} \times (\vec{B}_0)] \cdot \vec{W}^1 d\Gamma + \mathbf{S} A_r \end{aligned} \tag{77}$$

In order to get $SA_r$, the BEM system defined in equations (41) and (42) is solved :

$$\mathbf{P} k_r = \mathbf{D}(a - a_0) \tag{78}$$
$$\mathbf{S} a_r = \mathbf{Q} k_r \tag{79}$$

The coupled FEM-BEM system hence reads; similarly to Equations (48), (49) :

$$\mathbf{P} k^{t+1}_{r,(n+1)} = \mathbf{D}(a^{t+1}_{n+1} - a^0) \tag{80}$$
$$[\mathbf{M}^1(\sigma) + dt \mathbf{S}^1(\frac{1}{\mu})] a^{t+1}_{n+1} = \mathbf{M}^1(\sigma) a^t - dt \mathbf{Q} k^{t+1}_{r,(n+1)} + dt b^0 \tag{81}$$

with the two extra 1-form vectors :

$$
\begin{aligned}
a_i^0 &= \int_\Omega \vec{A}_0 \cdot \vec{W}_i^1 d\Omega && (82)\\
b_i^0 &= \int_\Gamma \frac{1}{\mu}(\vec{n} \times \vec{B}_0) \cdot \vec{W}_i^1 d\Gamma && (83)
\end{aligned}
$$

$a^0$ and $b^0$ can be directly computed if the external field is given as $\vec{B}_0(\vec{x}, t)$ (In which case, $\vec{A}_0$ has to be determined as $\vec{\nabla} \times \vec{A}_0 = \vec{B}_0$).
If the external field comes from a given current density distribution $\vec{j}_s(\vec{r})$, then $\vec{A}_0$ and $\vec{B}_0$ can be computed using the Biot-Savart law :

$$
\begin{aligned}
\vec{A}_0(\vec{r}) &= \frac{\mu_0}{4\pi} \int \frac{\vec{j}_s(\vec{r'})}{|\vec{r} - \vec{r'}|} d\vec{r'} && (84)\\
\vec{B}_0(\vec{r}) &= \frac{\mu_0}{4\pi} \int \frac{\vec{j}_s(\vec{r'}) \times (\vec{r} - \vec{r}')}{|\vec{r} - \vec{r'}|^3} d\vec{r'} && (85)
\end{aligned}
$$

## 4.3 With LS-DYNA's other solvers

### 4.3.1 Electromagnetic and structure interaction

The scope of the solver is not only to solve the Maxwell equations in the Eddy-current approximation but can also be coupled with the thermal and solid mechanics solvers of LS-DYNA in order to take full advantage of their capabilities. All materials available in LS-DYNA can therefore be used independently of their electromagnetic properties. The materials with strain rate dependency (ex: Johnson-Cook [9], Zerilli-Armstrong [23], Steinberg [19]) are particularly well suited for very fast deformation applications such as magnetic forming or welding.

The mechanical solver may run in explicit or implicit mode and the electromagnetism solver runs in implicit mode only as described in Equation (47). They both have distinct time steps and the EM fields are evaluated at the mechanical time step by linear interpolation. In typical EM forming and welding cases, the mechanical solver runs in explicit mode resulting in mechanical time steps that are a lot smaller than the electromagnetic time step. At each electromagnetic time step, the two solvers will interact. The electromagnetism solver will communicate the Lorentz force described in Equation (56) to the mechanical solver resulting in a extra force in the mechanic equation :

$$\rho \frac{Du}{Dt} = \nabla \times \ddot{\sigma} + f_{ext} + F_{Lorentz} \tag{86}$$

The mechanical solver will return the displacements and deformations of the conductors.

### 4.3.2 Thermal coupling

Both the thermal and the electromagnetism solver run implicitly. At each electromagnetic time step, the electromagnetism solver will communicate the extra Joule heating power term and the thermal solver will communicate the temperature. Several equations of state are implemented in the electromagnetism solver that permit to define how the conductivity is evolving as a function of the temperature :

- A Burgess model [3] giving the electrical conductivity as a function of temperature and density. The Burgess model gives the electrical resistivity vs temperature and density for the solid phase, liquid phase and vapor phase. For the moment, only the solid and liquid phases are implemented.
- A Meadon model giving the electrical conductivity as a function of temperature and density. The Meadon model is a simplified Burgess model with the solid phase equations only.
- A tabulated model allowing the user to enter his own load curve defining the conductivity function of the temperature.

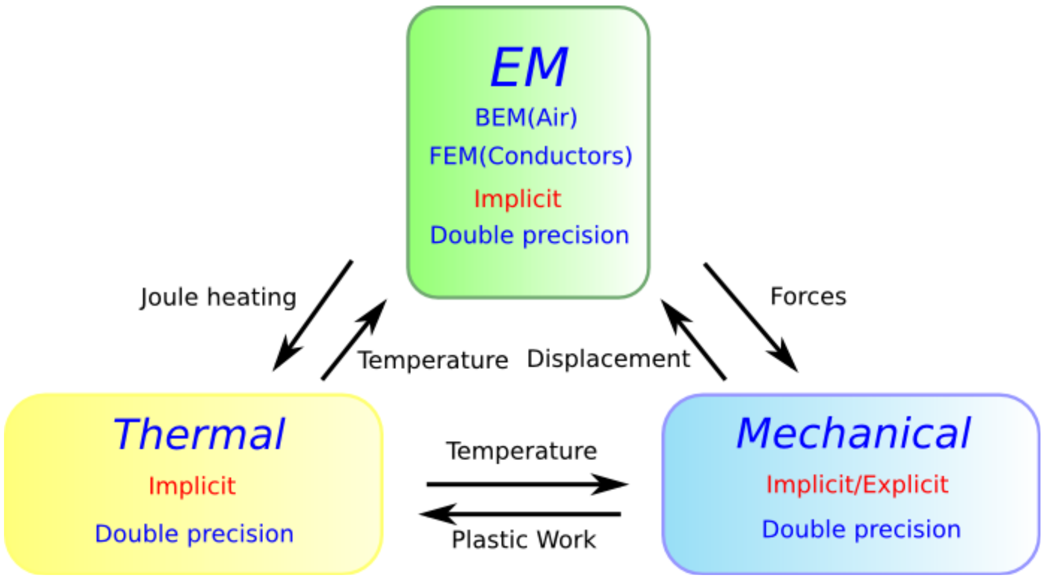


Figure 12: Interactions between the different solvers

# 5 Additional features of the solver

## 5.1 The inductive heating solver

Induction heating is the process of heating an electrically conducting object (usually a metal) by electromagnetic induction (usually with a moving or non-moving coil), where eddy currents are generated within the metal and resistance leads to Joule heating of the metal. The solver works in the time domain and not in the frequency domain, in order to easily take into account coil/workpiece motion as well as the time evolution of the EM parameters. Therefore, in order to solve an eddy current problem a EM time step compatible with the frequency (i.e. a time step such that there are at least a few dozens of steps in the period of the current) is needed. For example, with a frequency of 1MHz, a time step around 1.e-8 seconds would be needed and thus 1.e8 time steps to solve a full problem lasting 1s. Therefore, an induction heating analysis would be time consuming using the classic Eddy-current solver.

The induction heating solver works the following way: it assumes a current which oscillates very rapidly compared to the total time of the process (typically, a current with a frequency ranging from kHz to Mhz and a total time for the process around a few seconds). The following assumption is done: a full eddy-current problem is solved on a period with a "micro" EM time step. The user can specify the number of these "micro" EM step in a period. An average of the EM fields during this period as well as the joule heating are computed. It is then assumed that the properties of the material (and mostly the electrical conductivity which drives the flow of the current and the joule heating) do not change for the next periods of the current. These properties depending mostly on the temperature, the assumption can therefore be considered accurate as long as the temperature does not change too much. During these periods, no EM computation is done, only the averaged joule heating power is given to the thermal solver. But, as the temperature changes, and thus the electrical conductivity, the EM fields need to be updated accordingly, so another full eddy current resolution is computed for a period of the current giving new averaged EM fields and an update of the Joule heating power. The user can define this "macro" time step when the EM fields are recomputed on a new period (defined in the EM CONTROL or EM CONTROL TIME STEP cards). The solver can therefore efficiently solve problems involving inductive heating for a moving or non-moving coil.

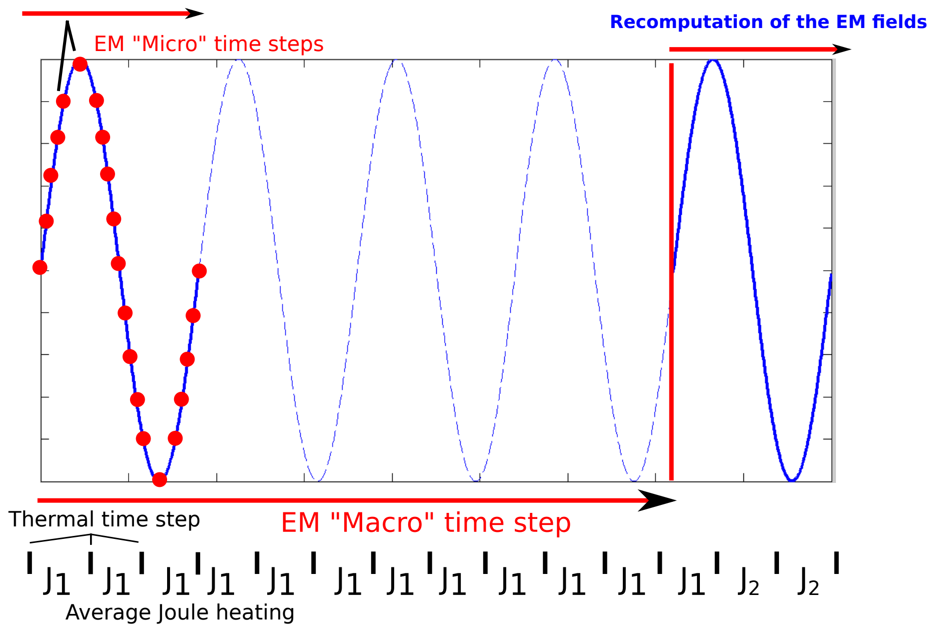


Figure 13: Inductive heating solver

## 5.2 The resistive heating solver

The resistive heating solver is a simplified version of the eddy current model where only resistive and no inductive effects are computed. The vector potential $\vec{A}$ is equal to zero all over and only the scalar potential $\Phi$ is kept. The equation system simplifies to :

$$S^0(\sigma)\phi = 0 \tag{87}$$

$$a = 0 \tag{88}$$

with mandatory Dirichlet and Newman conditions applied on the boundaries for Equation (87). Therefore only circuits that impose the tension can be used for this solver (Type 2-3-12 in the EM CIRCUIT card). There are no inductive effects since $\vec{A} = 0$, hence no coupling from a coil to the workpiece. This model is for very slow rising currents in a piece connected to a generator, where the diffusion and inductive effects can be considered as infinitely fast. The joule heating due to the current is still taken into account but no mechanical force is generated since $\vec{B} = \vec{\nabla} \times \vec{A} = 0$. Very large timesteps can be used and since $\vec{A} = 0$ and no BEM system is needed, this makes this solver much faster than the full eddy current model. After solving Equation (87), the EM fields result in :

$$\vec{j} = -\sigma \vec{\nabla}\Phi \tag{89}$$

$$\vec{B} = 0 \tag{90}$$

$$\vec{E} = -\vec{\nabla}\Phi \tag{91}$$

$$\vec{F}_{Lorentz} = 0 \tag{92}$$

## 5.3 Axisymmetric capabilities

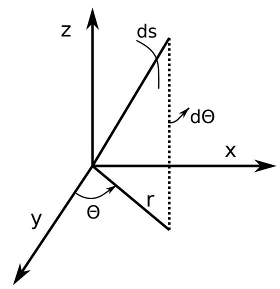


The axi-symmetric feature has been developed in order to simplify some cases and to save some calculation time. The electromagnetic 2D axi-symmetric feature is always coupled with the 3D thermal and structural solvers. The electromagnetic forces and Joule heating are calculated in 2D along the mid-plane of the axi-symmetric parts and are reported by simple rotations for coupling with the 3D mechanic and thermal. A future objective is to couple 2D axi-symmetric parts with classic 3D electromagnetic parts.

In the 2D- axi-symmetric case, the fields are independent of $\theta$ :

$$\vec{j}(r,\theta,z) = j(r,z)\vec{e}_\theta \tag{93}$$

$$\vec{A}(r,\theta,z) = A(r,z)\vec{e}_\theta \tag{94}$$

$$\vec{B}(r,\theta,z) = B_r(r,z)\vec{e}_r + B_z(r,z)\vec{e}_z \tag{95}$$

Equation (16) then reads [11] :

$$\sigma\frac{\partial A}{\partial t} - \frac{\partial}{\partial z}(\frac{1}{\mu}\frac{\partial A}{\partial t}) - \frac{\partial}{\partial r}(\frac{1}{\mu r}\frac{\partial(rA)}{\partial r}) = j \tag{96}$$

The 2D "1-form" basis function $\vec{W}^{'}$ is introduced such as : $\vec{W}^{'}(r,\theta,z) = W^1(r,z)\vec{e}_\theta$. This basis function can be seen as a 2d equivalent of a 0-form and is associated with the nodes. Equation (96) is projected against $W^{'}$ and after integrating by part one gets :

$$\begin{aligned}&\int\int \sigma W^{'}\frac{\partial A}{\partial t} rdrdz + \int\int \frac{1}{\mu r^2}[\frac{\partial(rW^{'})}{\partial r} + \frac{\partial(rA)}{\partial z}\frac{\partial(rW^{'})}{\partial z}]rdrdz = \\ &\int\int W^{'}jrdrdz + \int_\Gamma \frac{1}{\mu r}W^1\frac{\partial(rA)}{\partial n}rd\gamma\end{aligned} \tag{97}$$

With $\Gamma = \int ds$ the 1D boundary of the conductors and $\vec{n}$ the outer normal vector to $\Gamma$. In order to simplify the equations, the following change of variables is made :

$$A^{'} = rA \tag{98}$$

$$W^{"} = rW^{'} \tag{99}$$

then Equation (97) reads :

$$\int\int \frac{\sigma}{r} W" \frac{\partial A'}{\partial t} drdz + \int\int \frac{1}{\mu r}[\frac{\partial A'}{\partial r}\frac{\partial W"}{\partial r} + \frac{\partial A'}{\partial z}\frac{\partial W"}{\partial z}]drdz = \int\int W" jdrdz + \int_{\Gamma} \frac{1}{\mu r} W" \frac{\partial (A')}{\partial n} \tag{100}$$

which yields the matrix form similarly to Equation (33) :

$$\mathbf{M}^1(\sigma)\frac{\partial a'}{\partial t} + \mathbf{S}^1(\frac{1}{\mu})a' = \mathbf{S}a' \tag{101}$$

with :

$$\mathbf{M}^1(\sigma)(i,j) = \int\int \frac{\sigma}{r} W_i" W_j" drdz \tag{102}$$

$$\mathbf{S}^1(\frac{1}{\mu}) = \int\int \frac{1}{\mu r}[\frac{\partial W_i"}{\partial r}\frac{\partial W_j"}{\partial r} + \frac{\partial W_i"}{\partial z}\frac{\partial W_j"}{\partial z}]drdz \tag{103}$$

In order to compute $\mathbf{S}a'$ the BEM method is again introduced similarly to Equation (41) and (42) :

$$\mathbf{P}k = \mathbf{D}a \tag{104}$$

with :

$$\mathbf{P}(i,j) = \int ds_1 \int ds_2 \int d\theta_1 \int d\theta_2 \frac{\vec{V}_i(s_1,\theta)\cdot\vec{V}_j(s_1,\theta)}{||r_i(s_i,\theta_1) - r_j(s_2,\theta_2)||} r_1 r_2 \tag{105}$$

Since $\vec{V}_i$ and $\vec{V}_j$ do not depend on $\theta$ :

$$\mathbf{P}(i,j) = \int ds_1 \int ds_2 \vec{V}_i(s_1)\vec{V}_j(s_2) G(s_1,s_2) \tag{106}$$

with the axisymmetric 2D kernel :

$$G(s_1,s_2) = \int d\theta_1 \int d\theta_2 \frac{r_1 r_2}{||\vec{r}_1(s_1,\theta_1) - \vec{r}_2(s_2,\theta_2)||} \tag{107}$$

One can show that [11] :

$$G(s_1,s_2) = 4\pi\frac{\sqrt{r_1 r_2}}{k}[(1 - \frac{k^2}{2}L(k) - E(k)] \tag{108}$$

with :

$$
\begin{aligned}
d^2 &= (r_1 + r_2)^2 + (z_1 - z_2)^2 && (109)\\
k^2 &= \frac{4r_1r_2}{d^2} && (110)
\end{aligned}
$$

and :

$$E(k) = \int_0^{\frac{\pi}{2}} \sqrt{1 - k^2 sin^2\theta} d\theta \quad (111)$$

$$K(k) = \int_0^{\frac{\pi}{2}} \frac{d\theta}{\sqrt{1 - k^2 sin^2\theta}} \quad (112)$$

where $E(k)$ is a complete elliptic integral of second kind and $K(k)$ is a complete elliptic integral of first kind. Both are approximated by polynomials [6].

One can show that :

$$Q_{d_{i,j}} = 2\pi \int ds_1 ds_2 r_1 r_2 J \quad (113)$$

with :

$$
\begin{aligned}
J &= -\frac{a}{2r_1r_2d} K(k) + \frac{1}{2r_1r_2d}[2a + k^2(b-a)]\frac{E(k)}{1-k^2} && (114)\\
a &= w_1[z_n v_2(z_2 - z_1) - r_n r_1 v_2] && (115)\\
b &= r_n r_2 v_2 w_1 && (116)
\end{aligned}
$$

with :

$$
\begin{aligned}
\vec{w}_1(s) &= w_i \vec{e}_\theta && (117)\\
\vec{v}_2(s) &= -v_2 sin(\theta_2)\vec{e}_r + v_2 cos(\theta_2)\vec{e}_\theta && (118)\\
\vec{n}_x &= r_n \vec{e}_r + z_n \vec{e}_z && (119)
\end{aligned}
$$

All together, we end up with a system equivalent to Equation (48) and (49).

# References


[1] O. Biro and K. Preis, *On the use of the magnetic vector potential in the finite element analysis of three-dimentional eddy currents*, IEEE Transaction on Magnetics, 25 No. 4 (1989), pp. 3145–3159.

[2] A. Bossavit, *Computational electromagnetism*, (1998).

[3] T. Burgess, *Electrical resistivity model of metals*, 4th Int. Conf. on Megagauss Magnetic-Field Generation and Related Topics, Santa Fe, NM, USA, (1986).

[4] P. Castillo, R. Rieben, and D. White, *Femster: An object oriented class library of discrete differential forms.*, In Proceedings of the 2003 IEEE International Antennas and Propagation Symposium, 2 (2003), pp. 181–184.

[5] K. Chen, *On a class of preconditioning methods for dense linear systems from boundary elements*, 20 No.2 (1998), pp. 684–698.

[6] W. Cody, *Chebyshev approximations for the complete elliptic integrals k and e*, Mathematics of Computation, 19 No 89 (1965), pp. 105–112.

[7] F. Henrotte and K.Hameyer, *An algorithm to construct the discrete cohomology basis functions required for magnetic scalar potential formulations without cuts.*, IEEE transactions on magnetics, 39 No.3 (2003), pp. 1167–1170.

[8] J. Jin, *The finite element method in electromagnetics*, Wiley, (1993).

[9] G. Johnson and W. Cook, *Fracture characteristics of three metals subjected to various strains, strain rates, temperatures and pressures*, Engineering Fracture Mechanics, 21 No.1 (1985), pp. 31–48.

[10] W. K.F, S. R.H, and A. D.U, *Teaching electromagnetic field theory using differential forms*, IEEE Transactions on Education, 40 (1997), pp. 53–68.

[11] L. Pichon and A.Razek, *Hybrid finite-element method and boundary-element using time stepping for eddy current calculation in axisymmetric problems*, IEEE Proceedings, 136 No.4 (1989), pp. 217–222.

[12] H. P.J and S.Wylie, *Homology theory, on introduction to algebraic topology*, (1965).

[13] Z. Ren and A. Razek, *New technique for solving three-dimentional multiply connected eddy-current problems*, IEE Proceedings, 137 No.3 (1990).

[14] ——, *Computation of 3-d electromagnetic field using differential forms based elements and dual formulations*, International Journal of Numerical Modeling: Electronic Networks, Devices and Fields, 9 (1996), pp. 81–98.

[15] R. Rieben, *A Novel High Order Time Domain Vector Finite Element Method for the Simulation of Electromagnetic Devices*, PhD thesis, Universiy of California Davis, 2004.

[16] R. Rieben and D. White, *Verification of high-order mixed finite element solution of transient magnetic diffusion problems*, IEEE Transaction on Magnetics, 42 No.1 (2006), pp. 25–39.

[17] S. Sauter, *Cubature techniques for 3-d galerkin bem, boundary elements: Implementation and analysis of advanced algorithms*, (1996), pp. 29–44.

[18] J. Shen, *Computational electromagnetics using boundary elements, advances in modelling eddy currents*, Topics in Engineering 24 (1995).

[19] D. Steinberg, S.G.Cochran, and M.W.Guinan, *A constitutive model for metals applicable at high-strain rate*, J. Appl. Phys., 51 (1980), p. 1498.

[20] G. Vecchi, *Loop-star decomposition of basis functions in the discretization of the efie*, IEEE Transactions on Antennas and Propagation, 47 No.2 (1999).

[21] J. Volakis and D. Davidson, *Iterative-solver convergence for loop- star and loop-tree decompositions in method-of-moments solutions of the electric-field integral equation*, IEEE Transactions on Antennas and Propagation, 46 No.3 (2004), pp. 80–85.

[22] W. Wang and N. Atalla, *A numerical algorithm for double surface integrals over quadrilaterals with a 1/r singularity*, Communications in Numerical Methods in Engineering, 13 (1997), pp. 885–890.

[23] F. Zerilli and R. Armstrong, *Dislocation-mechanics-based constitutive relations for material dynamics calculations*, J. Appl. Phys., 61 No.5 (1987).

# A Consistent units for electromagnetism

| | USI | Equivalence ($[kg]^\alpha * [m]^\beta * [s]^\gamma$) | | | ex 1 | ex 2 |
|---|---|---|---|---|---|---|
| Mass | kg | $[kg]^\alpha$ | $[m]^\beta$ | $[s]^\gamma$ | g | g |
| Length | m | | | | mm | mm |
| Time | s | | | | s | ms |
| Energy | J | 1 | 2 | -2 | $1e^{-9}$ | $1e^{-3}$ |
| Force | N | 1 | 1 | -2 | $1e^{-6}$ | 1 |
| Stress | Pa | 1 | -1 | -2 | 1 | $1e^{6}$ |
| Density | $\frac{kg}{m^3}$ | 1 | -3 | 0 | $1e^{6}$ | $1e^{6}$ |
| Heat capacity | $\frac{J}{kgK}$ | 0 | 2 | -2 | $1e^{-6}$ | 1 |
| Thermal Cond. | $J\ m^{-1}s^{-1}$ | 1 | 1 | -3 | $1e^{-6}$ | $1e^{3}$ |
| Current | A | 0.5 | 0.5 | -1 | $1e^{-3}$ | 1 |
| Resistance | Ohm | 0 | 1 | -1 | $1e^{-3}$ | 1 |
| Inductance | H | 0 | 1 | 0 | $1e^{-3}$ | $1e^{-3}$ |
| Capacity | F | 0 | -1 | 1 | $1e^{3}$ | 1 |
| Voltage | V | 0.5 | 1.5 | -2 | $1e^{-6}$ | 1 |
| B field | T | 0.5 | -0.5 | -1 | 1 | $1e^{3}$ |
| Conductivity | $Ohm^{-1}m^{-1}$ | 0 | -2 | 1 | $1e^{6}$ | $1e^{3}$ |

Table 5: Consistent units for electromagnetism